HOKKAIDO UNIVERSITY

Title	Study on the dynamics and inheritance of mitochondria during conidiation in Pyricularia oryzae
Author(s)	Balagalle Rajapaksha Mudiyanselage Gonigoda Walauwe, Dineesha Nipuni Balagalla
Degree Grantor	北海道大学
Degree Name	博士(農学)
Dissertation Number	甲第14651号
Issue Date	2021-09-24
DOI	https://doi.org/10.14943/doctoral.k14651
Doc URL	https://hdl.handle.net/2115/83135
Type	doctoral thesis
File Information	ineesha_nipuni_balagalla.pdf

Hokkaido University Collection of Scholarly and Academic Papers : HUSCAP

Study on the dynamics and inheritance of mitochondria during conidiation in *Pyricularia oryzae*

(イネいもち病菌の分生子形成時のミトコンドリアの動態と伝搬に関する研究)

Balagalle Rajapaksha Mudiyanselage Gonigoda Walauwe Dineesha Nipuni Balagalla

Submitted to the Graduate School of Agriculture

Hokkaido University

June 2021

In Partial Fulfilment of the Requirement for the Degree of Doctor of Philosophy in Agriculture

CONTENTS

LIST OF FIGURES iii

LIST OF TABLES iv

ABSTEACT v

Chapter 1
GENERAL INTRODUCTION 1

Chapter 2
VISUALIZATION OF MOVEMENT OF MITOCHONDRIA IN *Pyricularia oryzae* USING CITRASE A – GFP 16
Introduction 16
Methodology 19
Results 21
Discussion 31

Chapter 3
ESTABLISHMENT OF REAL-TIME PCR PROTOCOL 33
Introduction 33
Methodology 35
Results 40
Discussion 43

Chapter 4
q-RT-PCR TO QUANTITY ISOLATES FOR THE HOMOPLASMY AND HETEROPLASMY CONDITION 44
Introduction 44
Methodology 47
Results 51
Discussion 52

Chapter 5
General Discussion 53

REFERENCES 56

ACKNOWLEDGEMENT 63

LIST OF FIGURES

Figure 1 Symptoms of *Magnaporthe oryzae* infection in rice 3

Figure 2 life cycle of the rice blast fungus *P. oryzae* 5

Figure 3: Single isolate can develop into blaso and gangliar conidia in *P. oryzae* 6

Figure 4: Blasto-conidia in *P. oryzae* 7

Figure 5 General functions of mitochondria 9

Figure 6 TCA cycle 11

Figure 7 The slide culture system 20

Figure 8 Representative series of observations observed under lower magnification (20X) 23-24

Figure 9 Mitochondrial movement and morphology during conidia 27-28

Figure 10 Mitochondrial movement and morphology during conidia development 29-30

Figure 11 Mitochondrial distribution during budding in *S. cerevisiae* 46

LIST OF TABLES

Table 1: Summary of the observations of mitochondrial movement into coniduim from condiaphore in *P. oryzae* 26

Table 2. Composition of reaction mixture for q-RT-PCR (SYBR Green ER qPCR SuperMix for ABIPRISM) 36

Table 3. Condition of reaction for qPCR (SYBR Green ER qPCR SuperMix for ABIPRISM) 36

Table 4. Composition of reaction mixture for qPCR (Go Taq qPCR Master Mix) 37

Table 5. Condition of reaction for qPCR (Go Taq qPCR Master Mix) 37

Table 6: Primer list for amplification of wild type and QoI resistant type of cyt b allele 39

Table 7 Mean total copy number of WT and MT alleles per total DNA 41

Table 8 WT and MT allele copy number per total DNA and WT / MT ratio in sensitive and resistant strains 42

Table 9: Enzyme reaction mixture 49

Table 10 q-RT-PCR conditions 50

Table 11 Primer list for amplification of wild type and QoI resistant type allele 50

Table 12 Ratio between wild type allele and resistant allele in colonies with *P. oryzae* with conidiation and with no-conidiation 51

ABSTRACT

Pyricularia oryzae, which causes rice blast disease in rice, is a filamentous ascomycete fungus. QoI fungicide (quinone – outside inhibitors) is one of the major fungicides to control rice blast disease. They inhibit mitochondrial respiration by binding to the Q_o site of the cytochrome (bc1) enzyme complex, blocking the electron transport chain and consequently reduce the production of ATP. In recent decades, resistance has been developed for this fungicide due to single nucleotide substitution in *CytB* gene in mitochondrial DNA (mtDNA). Therefore, it is important to understand mitochondrial dynamics and inheritance to curb the resistance development in the fungus. In this study, visualization of GFP-fused mitochondria was used to understand the movement and shape of the mitochondria during the initial stage of conidia formation. In addition, wild and the mutant allele were quantified using quantitative PCR (qPCR) to understand the process of homoplasmy during conidiation.

1. Microscopic observation of mitochondria dynamics in the initial stage of conidiation

The movement and shape of the mitochondria during initial stages of conidiation were investigated using *P. oryzae* transformant harboring GFP-tagged Citrate synthase (Cit A) gene. Strain Ina86-137 CitA-GFP was cultured on special slide, with a thin paper soaked with oatmeal agar at 25ºC for 30-33hours. Observations were made every 20-30 minutes to investigate the movement and the shape of the mitochondria. It was observed that there is continuous flow of mitochondria from conidia to conidiophore during early conidiation. The shape of the mitochondria was initially tubular at zero minute of observation and later they changed into dot shape at around 100-120minutes before the flow of the

mitochondria stops. Septa formation was also observed parallel to development of dot shaped mitochondria.

It is very important to understand about the shape and movement of mitochondria during conidiation to introduce novel strategies to control rice blast disease.

2. Establishment of qPCR for the quantification of *Cytb* alleles in mtDNA

One nucleotide substitution in the cytochrome b (*Cytb*) gene had been revealed to develop resistance against QoI fungicides. Absolute qPCR system was established to quantify each *Cytb* allele in this study, in order to monitor the ratio of resistant and wild type allele in a strain. A linear standard curve was produced using standard DNA clone of each allele, for 10^8-10^4 copies. Two resistant (R) field isolates and one susceptible field isolate (S) were collected from each Akita and Hyogo prefectures. They are namely, 2013-156 (R), 2013-131(R), 2013-208(S) and 128(R), 132 (R), 130(S). The quantity of the alleles were measured using qPCR and ratio of resistant and wild type allele were calculated. The WT : MT ratio of the resistant strains, 2013-156, 2013-131, 128r, and 132r were 1 : $1.05x10^3$, 1 : $2.02x10^3$, 1 : $7.76x10^2$, and 1 : $272x10^3$ respectively. In the susceptible strains 2013-208 and 130s the WT : MT ratio was $5.21x10^2$: 1 and $9.07x10^2$: 1 respectively. The quantity of the MT allele of the resistant strains was higher compared to the WT alleles. In the susceptible strains the quantity of WT allele was higher compared to the MT allele.

3. Elucidation of relationship between conidiation and homoplasmy

Occurrence of mutation in mitochondria will lead the heterogeneity of mitochondria in a cell, which is called heteroplasmy. Heteroplasmy is not stable, and often return to the condition called homoplasmy, in which one type of mitochondria dominates in a cell.

Occurrence and rapid spread of QoI resistant mitochondria in the wild population can be considered as a result of homoplasmy, but no investigation on the process to be homoplasmy in *P. oryzae*. In order to study about homoplasmy and a conidiation, a artificial heteroplasmy strain having similar amount of wild type allele and mutant allele *Cytb* mtDNA was produced using PEG-mediated protoplast fusion. This heteroplasmy was then used to generate single colony isolates with conidiation and without conidiation, by single conidia isolation and single protoplast isolation, respectively. The isolates with conidiation showed homoplasy when the quantity of the alleles were measured using qPCR. Those isolates had almost only the wild type allele. Isolates without conidiation retained heteroplasmy. These results suggested that conidiation is acting as an important process to maintain homoplasmy of mitochondrial DNA.

This study demonstrated that the conidiation, which is an important event for *P. oryzae* which produces the cell required for the pathogenesis, is the key event for the spread of QoI resistance as well. Further analyses using qPCR system for *CytB* alleles and fluorescent microscopic observation of mitochondria may help to mitigate building-up of QoI fungicide resistance in *P. oryzae* and will have a great impact on the developing sustainable management practices against the rice blast disease in the future.

Chapter 1

GENERAL INTRODUCTION

Pyricularia oryzae, which causes rice blast disease in rice is a filamentous ascomycete fungus. *P.* oryzae is also the causal agent of blast disease of many cereals (Fernandez and Orth, 2018). This pathogen has a host range of over 50 species including many economically important cereals and grasses (Schulze-Lefert and Panstruga, 2011). According to Nalley et al., 2016, around 30% global rice production is loss due to rice blast, which is equivalent of feeding 60 million people annually. More than 55% of the world population lives in Asia and around 92% of the rice grown and consume rice (Barker et al, 1985). According to the analysis done by International Food Policy Research Institute, there is 3% increase in the rice demand in every year and there will be 38% increase by 2030 (Wilson and Talbot, 2009). China, Korea, Japan, Vietnam and United States had to destroy 5.7million hectares of rice in 2001 to 2005 due to rice blast disease (Wilson and Talbot, 2009).

In recent years, *P. oryzae* has attracted attention of many researchers due to its economic importance and as a model organism to investigate plant diseases. Therefore, detailed information of different strains of *P. oryzae* and sequence data of the genome has become wildly available (Chen et al, 2020; Wilson and Talbot, 2009; Zhu et al, 2016). *P. oryzae* can infect leaves, stems, nodes and panicles of rice which include all stages of development of the plant (Fig 1a-c). It was found that this fungus can even infect roots of the rice plant (Sesma and Osbourn 2004). Upon infection in rice seedlings, small lesions

with a necrotic centre and a chlorotic margin are visible on leaves (Rahnama et al, 2020). The major economic damage is caused by the neck and panicle blast which occurs in the reproductive stage of the rice plant (Fig. 1b). This can drastically reduce the grain yield per plant. On mature leaves large lesions with a necrotic centre and a chlorotic margin are visible (Fig. 1c).

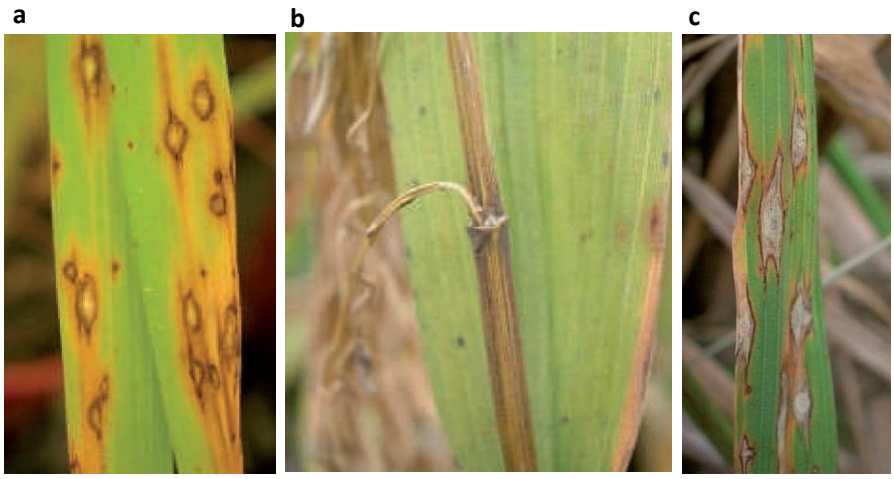

Figure 1 Symptoms of *Magnaporthe oryzae* infection in rice. **a,** Rice blast affects seedlings, causing a leaf spot disease characterized by spreading lesions with a necrotic centre and a chlorotic margin. **b,** In the field, neck and panicle blast are the major causes of rice yield losses. The fungus sporulates profusely at nodes on the rice stem and rots the neck of the mature rice plant, either causing the panicle to be lost or preventing grain filling and maturation. **c,** Large rice blast lesions, which can be more than 1 cm in length, on a mature rice plant. *P. oryzae* sporulates from lesions, and spores are dispersed by dewdrop splash. Images are from Wilson and Talbot (2009).

Life cycle of *P. oryzae*

P. oryzae has seven chromosomes and a genome size of 40Mb, with approximately 9,000 genes. The pathogen cause blast spots on infected plants and aerial conidiophores emerge from the conidia on the centre of the lesions which develops into a haploid ascomysete (Boddy, 2016). *P. oryzae* undergo series of developmental stages to infect the host plant. Initiation of infection happens when the three celled tear drop-shaped conidia attached to the rice leaf cuticle. The conidia contain glycoprotein which becomes adhesive when wet and helps to stick to the leaf surface. This aids the conidia to be spread with the help of rain and wind and usually outbreak during rainy season or transition to rainy season (Asibi et al. 2019; Dean et al, 2005). Upon a conidium stick on to a leaf tissue, one of the terminal cells start germinating rapidly and produce germ tube to consequently penetrate the leaf cuticle. Thus, the apex of the germ tube becomes swollen and flattened developing into an appressorium. An appressorium is a specialized cell with a melanin-lined thickened cell wall (Perez-Nadales, 2014). A penetration peg is produced at the bottom of the appressorium which penetrates the leaf surface and enters the cell. This leads to a successful infection of *P. oryzae* and new disease lesions will become visible about 4 days after inoculation (Fig. 2).

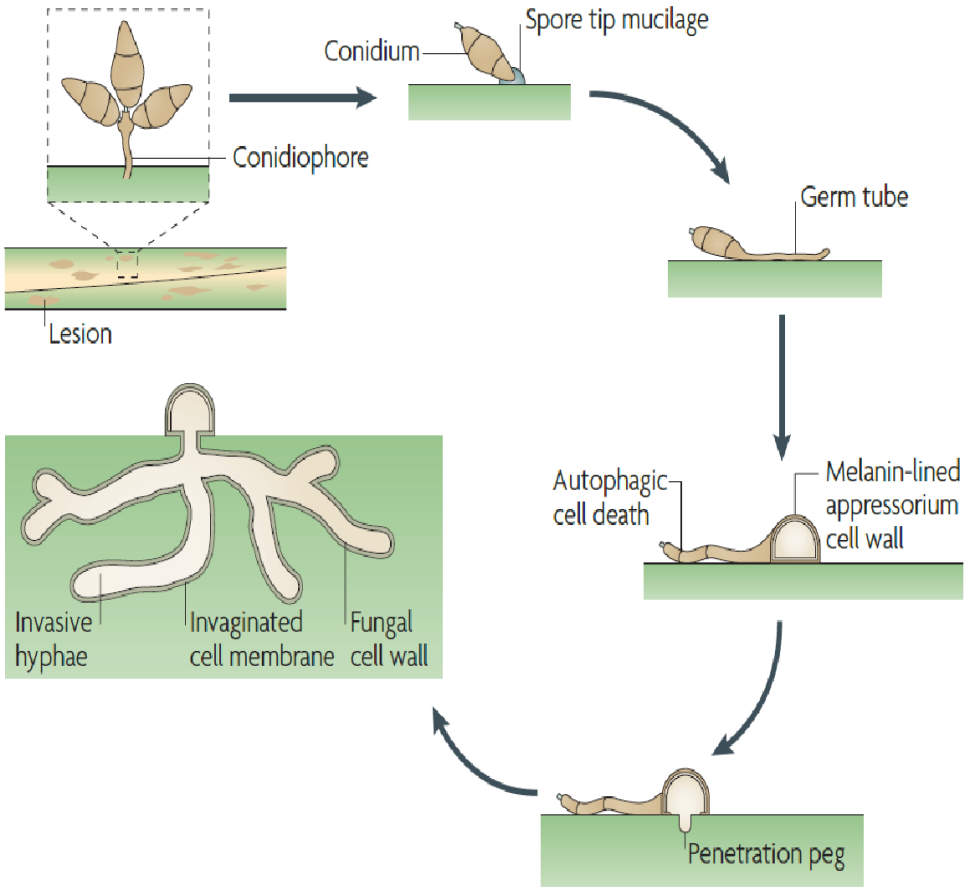

Figure 2 life cycle of the rice blast fungus *P. oryzae* (Wilson and Talbot, 2009).

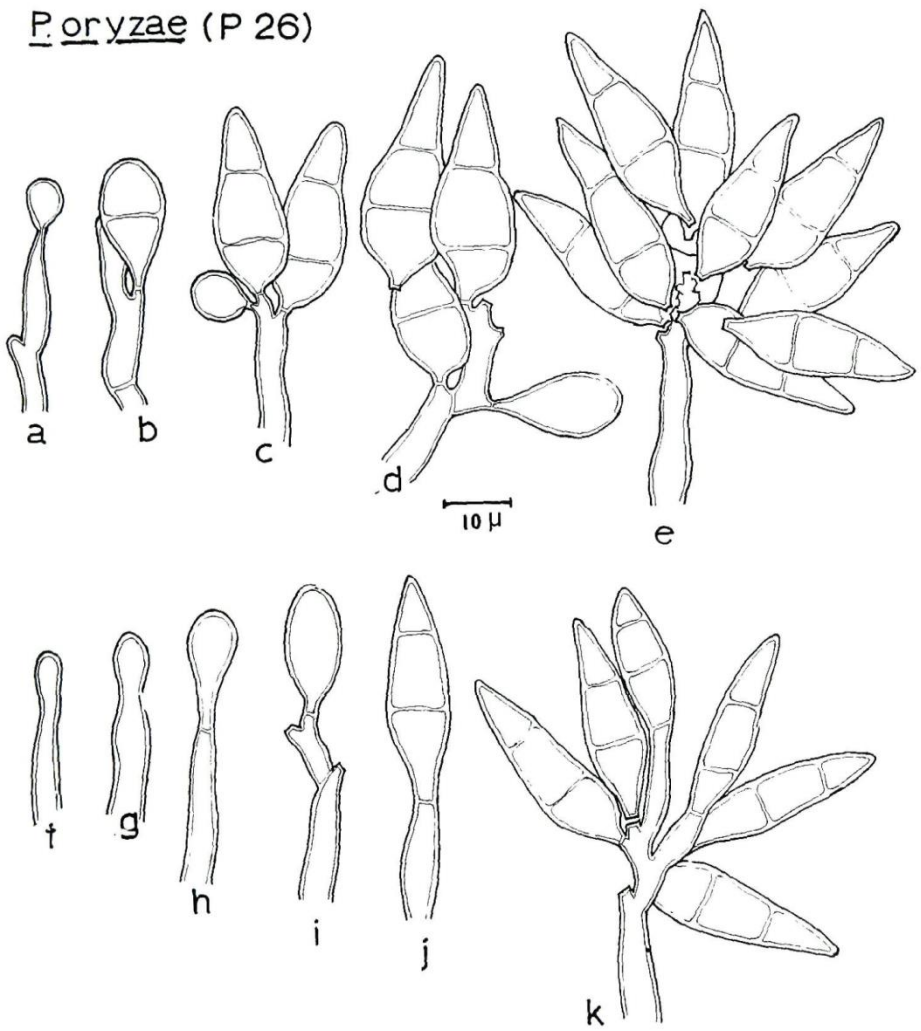

Figure 3: Single isolate can develop into blaso and gangliar conidia in *M oryzae*. **a-e,** development of blastoconidia. Blastoconidia generally detached at the conidiophore when they become mature. **f-j,** development of gangliar conidia. They remain attached to the conidiophore when they become mature (Rao and Jesudhas, 1984).

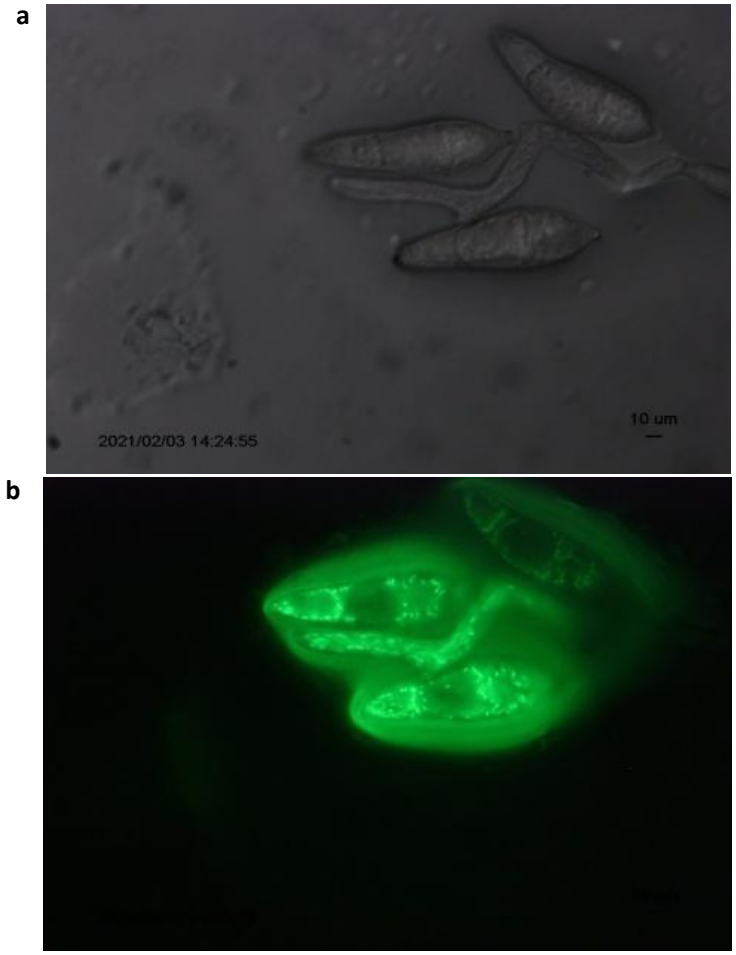

Figure 4: Blasto-conidia in Ina 86 137. The mature conidia are detached from the conidium. **a,** Images taken under bright field lens **b,** Images taken under fluorescence lens

There are two types of conidiation in *P. oryzae,* namely blasto and gangliar (Fig 3). Protuberance will arise at the tip of the conidiophore and it appears like a narrow constriction. Later the three celled conidia will be formed and it will develop its shape and size (Rao and Jesudhas, 1984). Blasto-conidia in *P. oryzae* when mature conidia are detached from the conidium is shown in Fig 4.

Mitochondria

Emergence of mitochondria in a cell was described as an adaptation to deal with oxygen in atmosphere (Sagan 1967). In general, Mitochondria are called as the power house of a cell. Mitochondria, the main generator of adenosine triphosphate (ATP) are a semi-autonomous double-membrane bound organelle. ATP is important for diverse cellular functions which ultimately result in various physiological processes such as redox signalling, homeostasis, lipid metabolism and programmed cell death. Mitochondria have more importance in recent decade because it performs various functions other than ATP and macromolecules production. Furthermore, mitochondria have role in cell homeostasis by involving in signalling events namely, release of cytochrome c to invoke caspase-dependent cell death, release of reactive oxygen species to oxidize thiols within redox-regulated proteins, and induce gene expression and the activation of AMPK under energetic stress to control mitochondrial dynamics (Martínez-Reyes, I. and Chandel, N.S., 2020). The graphical representation of the general functions of mitochondria is given in Figure 5.

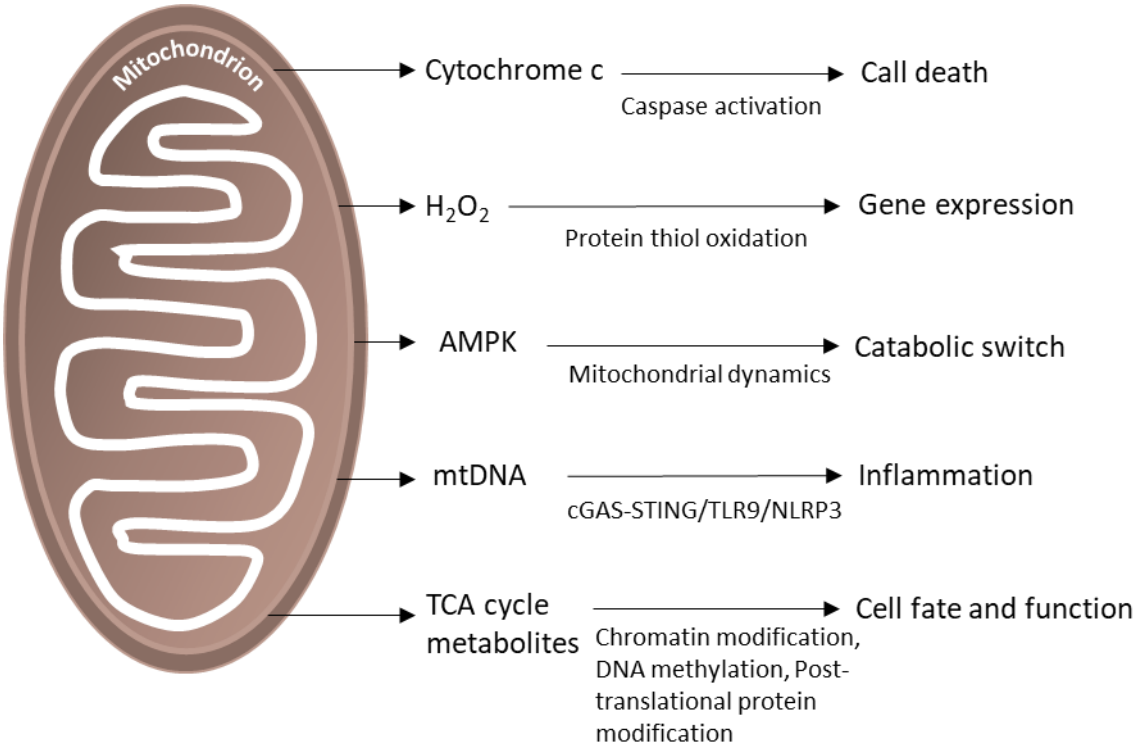

Figure 5 General functions of mitochondria.

TCA cycle

Mitochondria provide chemical energy for the cell in the form of ATP produced through the TCA cycle. Respirosomes are supercomplex molecules (complex I, III and IV) which are present in inner mitochondrial membrane to carry-out the oxidation process. They oxidize NADH and transfer electrons to final electron acceptor (oxygen). Electron transport chain results in proton motive force across mitochondrial membrane into inter-membrane space which will provide flow of protons for the generation of ATP (Figure 6).

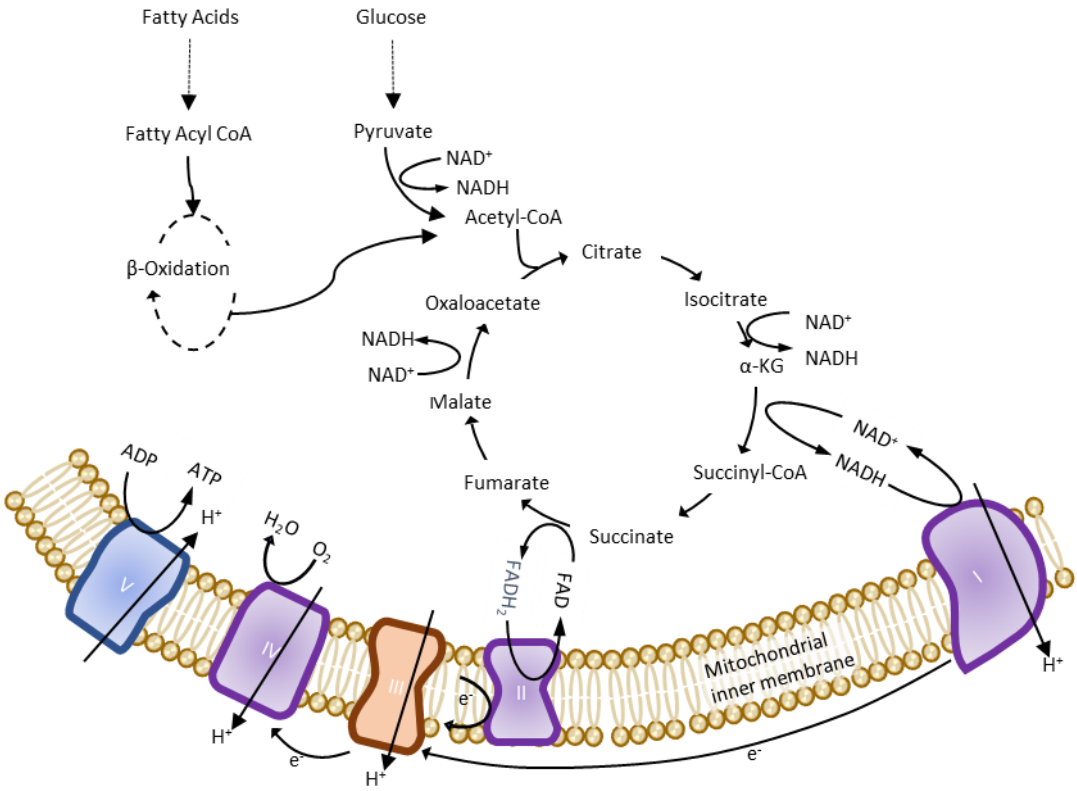

Figure 6 TCA cycle. In a series of enzymatic reactions, electrons are transferred to the electron transport chain (ETC) which is known as the mitochondrial respiratory chain.

Mitochondrial DNA

Mitochondrial DNA (mtDNA) can be defined as DNA present in mitochondrion and also additional DNA types (small linear plasmid-like DNA) that are present in the mitochondria. These DNA can replicate independently and contains protein–encoding genes that are responsible for respirasome production. Conversely, there has to be compatibility between nuclear encoded and mitochondrially encoded components for the proper function of mitochondria. mtDNA is more prone to mutations than that of nuclear DNA but they lack efficient repair mechanism in them. There can be simultaneous mutations in different Mt DNA, thus it might surpass the wild type mtDNA (Mendoza et al 2020).

Fusion and fission

Fusion and fission in mitochondria is a continuous process which occurs during its growth. These two opposing processes give a dynamic shape to mitochondria which leads to a variety of morphologies. Mitochondrial number is also regulated by fission and fusion process and these processes can determine the number of mitochondria per cell at any specific time. It is linked with development process like cell cycle as well. These processes have role in mitochondrial structural integrity, function and appropriate distribution into cells and helps cells to adapt to the environment context. Therefore, mitochondria morphology is also highly dynamic and can range from elongated or interconnected networks spanning the whole cell (Westermann, 2010). Mitochondria exchange both soluble and membrane components during fission therefore they can repair "transient defects" through this process (Lackner 2014).

There are molecules called as “dynamins” which are superfamily GTPase proteins (DRPs). They are found in rice blast fungus and further studies have shown that MoDnm1, MoFis1 and MoMdv1 are in complex to regulate mitochondrial fisson, mitophagy progression and appressorium function and host penetration (Zhong et al 2016). Dnm1 is present in cytosol and it must be delivered to mitochondrial outer membrane for proper function (Bui et al 2012) and it is involved to maintain equilibrium between fission and fusion (Westermann 2010). Recent research evidence suggest that Dnm1 is the master regulator of mitochondrial division (Zhong et al 2016).

Autophagy and mitophagy

Autophagy and mitophagy are crucial cellular processes that are responsible to maintain cell equilibrium and these processes can selectively eliminate dysfunctional organells (Youle and Narendra 2011). The main role of mitochondria in conidia is to provide the energy for germination and growth before the host is parasitized (Li and Calderone 2017). There is a transition period from biotrophy to nectrotrophy in *M oryzae* and during this period mitochondrial dynamics and mitophagy is crucial (Kou et al 2019). Mitochondria in conidia have a much more important role in germination and growth before the fungus has completely transformed into nectrotrophy (Li and Calderone 2017).

QoI fungicide (Strobilrin fungicide)

QoI fungicide (quinone – outside inhibotors) are most important class of fungicide and it is recorded as highest selling fungicide in the world (Ishii 2006). They inhibit mitochondrial respiration by binding to the Qo site of the cytochrome (bc1) enzyme complex. It will block the electron transfer and then block the production of ATP. This fungicide is specific for single binding site and therefore they have high probability of the developing fungicide resistance.

In recent years, *M oryzae* has undergone single nucleotide mutation at cytochrome b (*cyt b*) gene that prevents the binding of the fungicide at Qo site. Further, they have developed fungicide resistance by undergoing single nucleotide substitution at the same site, from glycine to alanine at position 143 (G143A) or from phenyl alanine to leucine at position 129 (F129L) (Castroagudín et al 2015).

In the last decade, monitoring QoI fungicide resistance was started in Japan. It has been identified that the QoI fungicide sensitivity of rice blast fungus has lost in some rice-growing areas in Japan (Ishii 2015). In 2012 in Japan the emergence of a QoI resistant strain in *P. oryzae* was detected in three prefectures, Yamaguchi, Shimane, and Ehime. Resistance was showed to the metominostrobin, orysastrobin and azoxystrobin which were all QoI fungicides (Miyagawa et al, 2013). In Brazil, QoI resistant *P. oryzae* was reported due to a single amino acid substitution, at position 143 (G143A) and this resistant population increased from 36% to 90% in 2005 to 2012 (Castroagudín et al. 2015). After discontinuance of QoI fungicides in Japan the frequencies of QoI resistant strains reported to be decreased significantly (Hayashi et al. 2017).

Strobilurins have become ineffective to control *M oryzae* infection during past decades due to few reasons. Main reason could be incomplete understanding of pathogen's life cycle and extensive usage for decades to control the fungal infection.

Chapter 2

VISUALIZATION OF MOVEMENT OF MITOCHONDRIA IN *Pyricularia oryzae* USING CITRASE A – GFP

2.1. Introduction

2.1.1 Microscopic observation

Microscopic observations are the best way to evaluate entire mitochondria with each aspect. The two basic types of microscopy are light microscope or electron microscope and they have their own advantages and disadvantages in visualization of mitochondria. There are few methods to measure the cellular mitochondrial content but 3D imaging is the only way to directly assess the volume of a cell that is occupied by mitochondria. 3D visualization is helpful to understand more about mitochondria without any blind spots (Syib'li et al 2020). There are few methods to visualize mitochondria under microscope, namely, 1. Label mitochondria in live cells using fluorescent dye; 2. Use mitochondria specific fluorescent antibodies; 3. Label with genetically encoded fluorescent dyes (Glancy 2020). Mito Tracker series of dyes work by binding to thiol groups within mitochondria and green fluorescent and MitoTracker can colocalized inside conidia (Syib'li et al 2020). The first report of the use of GFP as a mitochondrial marker was published in 1995 (Rizzuto et al 1995). The importance of visualizing mitochondria is that the number of mitochondria in a live cell is directly proportional to the cellular capacity of mitochondrial function (Glancy 2020).

2.1.2 GFP (Green Fluorescence Protein)

GFP was first cloned by Prasher (Prasher 1992) from jellyfish Aequorea victoria. This protein has very unique characteristics such as 238 amino acid, 27-kDa protein which absorbs light at maxima of 395 and 475 nm and emits light at maximum of 508 nm. It does not need any cofactor or substrate for its activity and it is proven to be stable *in vivo* (Lorang et al 2001). It can be fused to C or N terminus of many cellular and extra cellular proteins without loss of activity.

GFP has been expressed and used in many organisms as a reporter for gene expression and as a fluorescent tag for monitoring the subcellular localization in living cells (Kain et al 1955).

2.1.3 Conidiation/ Conidiogenesis

Conidia are also called as asexual spores and are involved in the disease cycle of the fungus. Hydration is the most important factor for this fungus to attach to the host plant and to produce germ tube. This fungus develops a specialized infection structure known as appressorium which generates the turgor pressure needed for penetration through host cell. Once the invasive hyphae are developed, it will colonize and produce massive conidia. This is known as the 'infection cycle' and may occur many times during the growing season. Cascade of morphological events are involved in Conidiation and *P. oryzae* produces three celled conidia through conidiation. It was shown that some mutants of *P. oryzae* has different ability to conidiate at different timings (Han et al 2018).

2.1.4 Mitochondria in conidia

Mitochondria in conidia were visualized using confocal microscope and mitochondria have different shapes based on length such as dots, tubules and network (Syib'li et al 2020). A novel version of mitograph was developed to quantify mitochondrial content in living cells (Viana et al 2015) and it was used to quantify mitochondrion at the hyphal tip. Dot shaped mitochondria were observed in hyphal tips and older hyphae had tubule shaped mitochondria (Syib'li et al 2020). It was observed that mean volume of mitochondria observed at the tip of hyphae is always smaller than the basal part (Syib'li et al 2020).

Recently, the emergence of a QoI resistance by a single point mutation at cytochrome b (*Cytb*) gene in *P. oryzae* was detected and has been widespread in Japan (Miyagawa et al. 2013; Ishii 2015; Castroagudín et al. 2015). On the other hand, after discontinuance of QoI fungicides in Japan the frequencies of QoI resistant strains reported to be decreased significantly (Hayashi et al. 2017). In order to clarify the mechanism of this phenomenon, it is necessary to characterize mitochondrial behavior of *P. oryzae* especially during the early stages of conidiation.

It is very important to understand the molecular mechanism involved in conidiation and mitochondrial distribution to introduce novel strategies to control rice blast disease.

2.2 Methodology

2.1.1 Preparation of slide culture

The filter papers were prepared (Figure 7a) and autoclaved. In order to characterize the mitochondrial movement and morphology during early conidiation, *CitA-GFP* fused strain (Syib'li et al. 2020) cultured on the filter paper soaked with oatmeal agar media were used. Thin filter paper (20 mm × 25 mm) was cut into the shape shown in figure7a and was soaked with the agar media. This filter paper was placed on a glass slide and pressed with coverslip to spread of the media evenly. Small piece of filter paper (5 mm ×5 mm) pre inoculated with the fungus was used for the inoculation. Later, it was covered with a coverslip. To prevent the filter paper from drying the coverslip and the filter paper was sealed using 'Vaseline'. The glass slides were placed on several toothpicks, inside a petri dish as shown in figure 7b and incubated at 25°C for 30-33 h. The humidity was maintained in the slide by adding water into extra filter paper placed on the slide.

The slides were observed under fluorescence microscope at 20X and 100X. The images were captured under bright field and fluorescence light. The system used was fluorescence microscope (Olympus BX 50) and all images were taken at bright field and fluorescence light in 20-30 minutes of time laps.

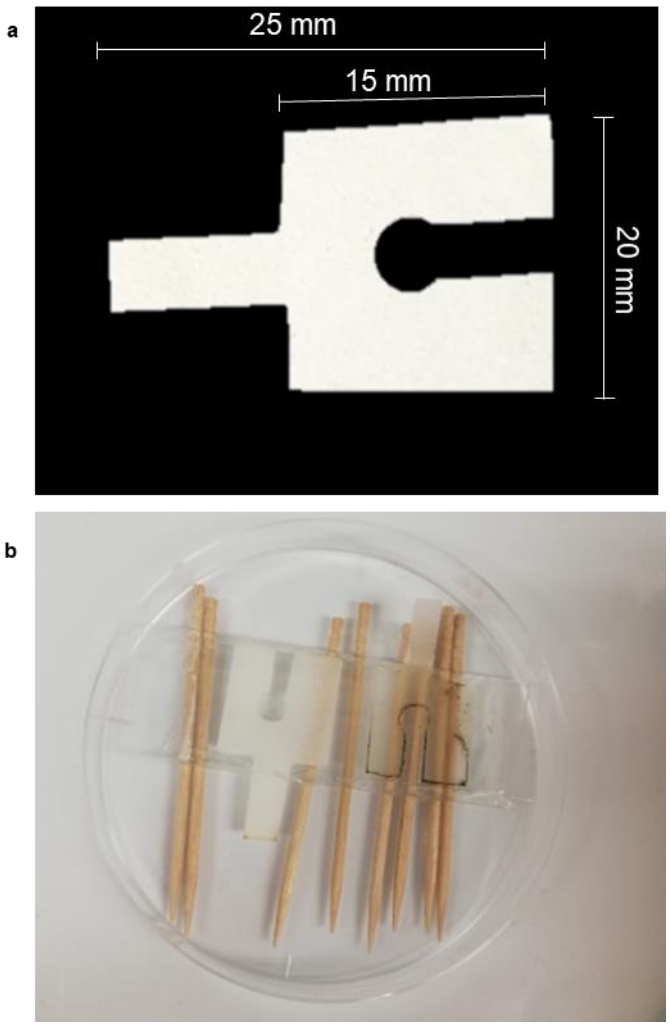

Figure 7 The slide culture system. **a.** shape and size of the filter paper **b.** arrangement for incubation of the culture by placing the glass slide on toothpicks inside a petri dish.

2.3 Results

For the mitochondria observation during conidiation initiation, periodical observations were made. Initially the observations were under lower magnification (20X) magnification. Four observations were captured periodically in time intervals in lower magnification to optimize the timing and observation point in the hyphae. One representative series of observations were shown in figure 8. Observations were made around every 25minutes till the conidia turn into two celled conidia using lower magnification. Development of protuberance from conidiophore was easily distinguishable under lower magnification. It was not easy to observe the shape and moment where the flow of the mitochondria stops under this magnification.

Later, the observations were made under higher magnification (100X). The first observation was taken when the protuberance like structure appears and terminated when two celled conidium was formed. The observations were made until the flow of the mitochondria from conidiophore to baby conidia stopped. At the initial stage (= time 0), it was observed that the tubular-shaped mitochondria were flowing continuously towards the edge of the protuberance (Fig. 9a, Table 1). After 28 minutes from the initial observation, formation of small circular shaped conidia was observed and the mitochondria were moving into the conidia and the shape remained as tubular (Fig. 9b, Table 1). At the third observation point (56 min after initial observation), the tubular mitochondria was still continuous from conidiophore to the conidia (Fig. 9c, Table 1). The shape of the conidium was circular throw-out the 56 minutes observation period but the size was increased with time. At 86 min after initial observation, the shape of the conidium changed into oval shape while it was observed that the mitochondria were still moving into the conidium. Yet the shape of the mitochondria was not changed (tubular

shaped). In addition, it was also observed that the mitochondria have distributed throughout the conidium (Fig. 9d, Table 1). The shape of the mitochondria started to change into dot after 100 minutes from the initial observation (Fig. 9e, Table 1). At this point, the flowing of mitochondria into the coniduim was stopped. Further, during this period septa formation was also observed. After around 100 minutes, the movement of mitochondria was completely stopped and in the next 20-30 minute the single cell conidium was turned into two-celled conidium. Septum was formed at the same observation point when the movement of mitochondria stopped. Similar observations observed in a separate conidiation is showed in figure 10.

Bright field

Flouracence light

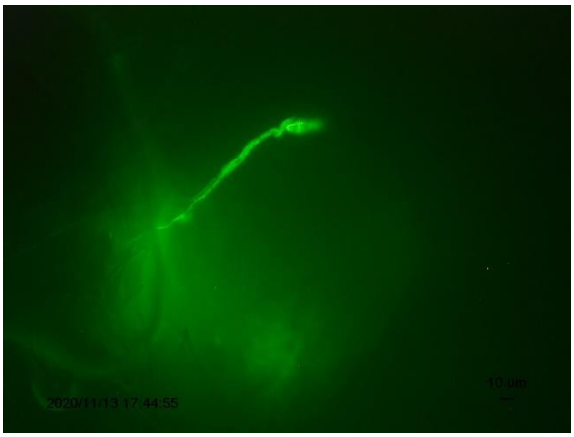

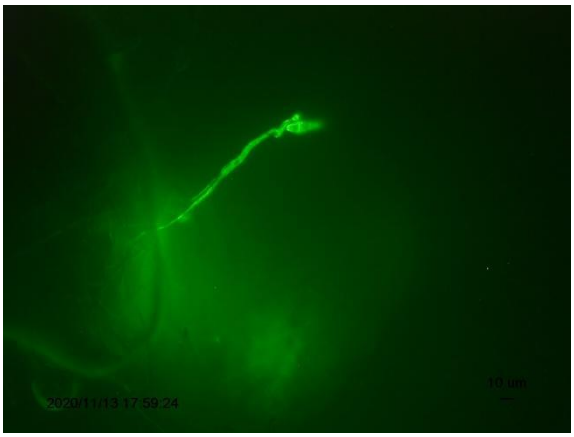

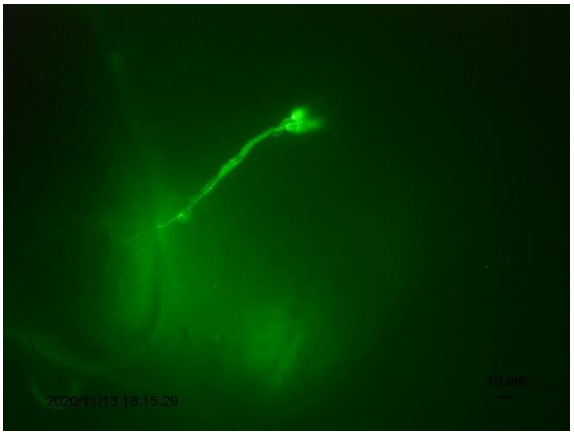

10 um
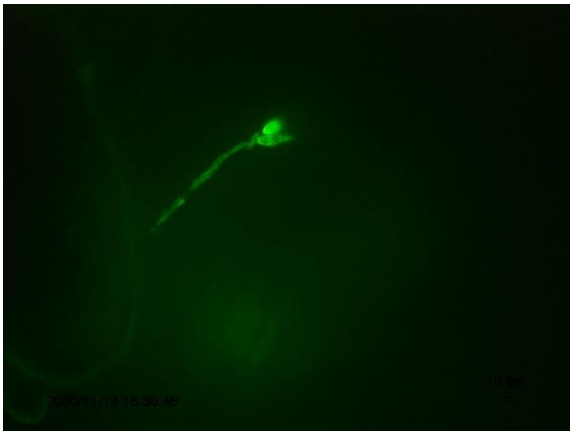
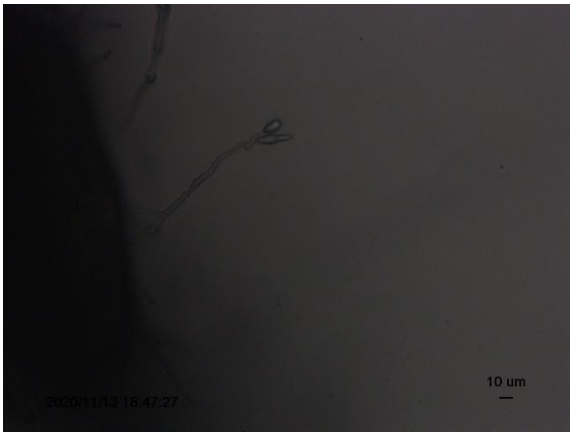
10 um
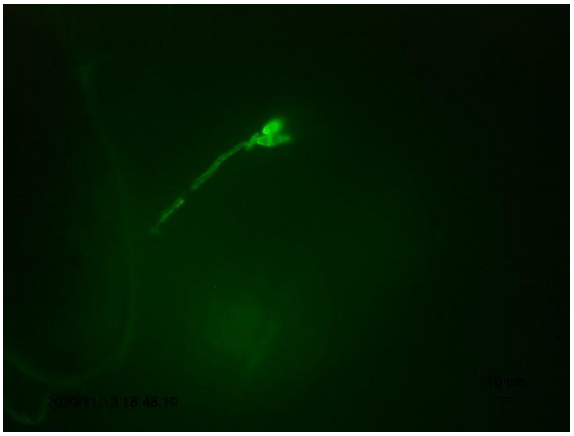

10 um
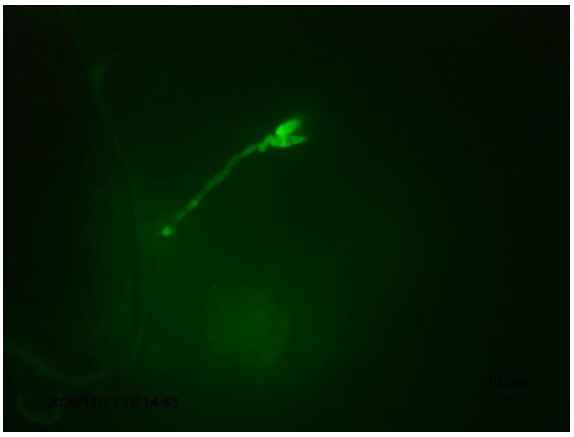

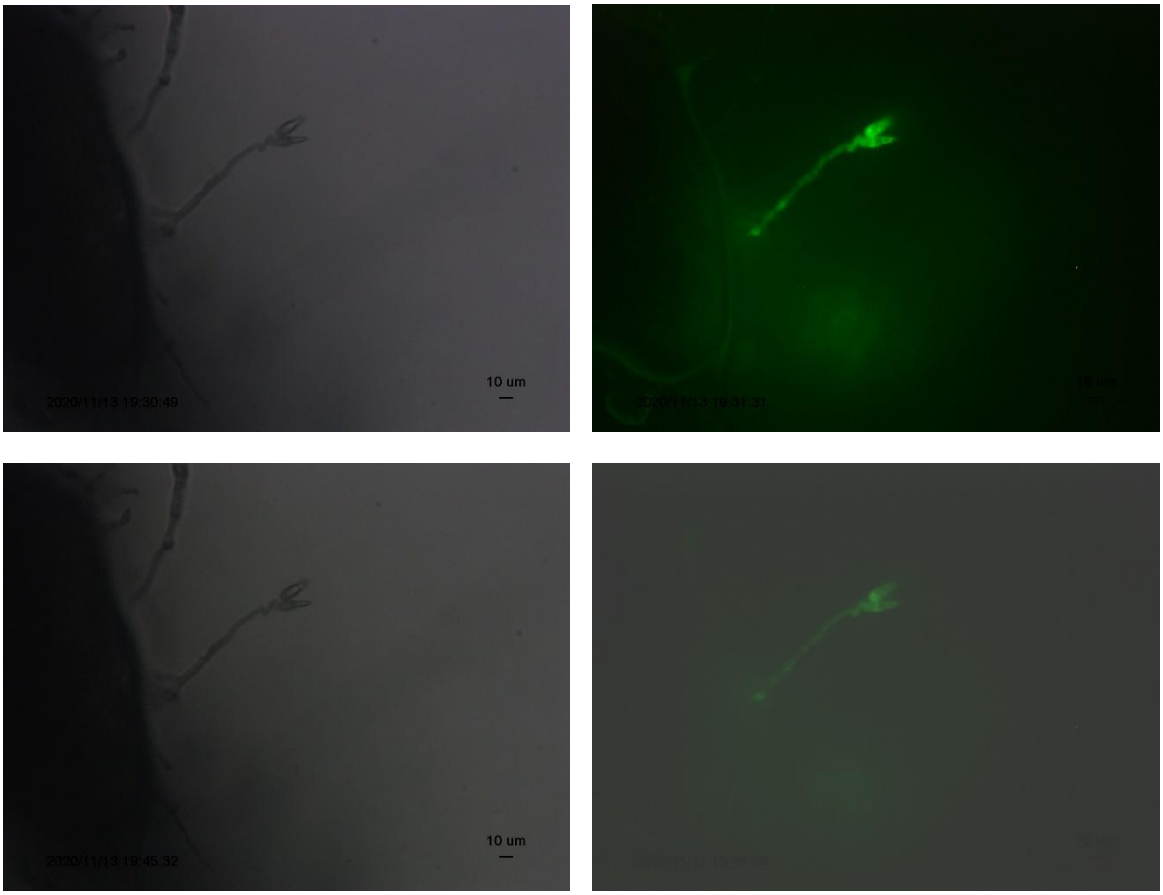

Figure 8 Representative series of observations observed under lower magnification (20X). Observations were captured periodically in time intervals to optimize the timing and observation point in the hyphae.

Table 1: Summary of the observations of mitochondrial movement into coniduim from condiaphore in *P. oryzae*

Average time[a] (Minutes)	Observation
0	protuberance like structure appears
25	Tubular shaped mitochondria, coniduim is circular in shape
50	Tubular shaped mitochondria, coniduim is circular in shape
75	Shape of the coniduim changed into oval
100	Dot shaped mitochondria, flowing of the mitochondria stopped. Formation of septa

[a]Average time was calculated based on eight individual observations

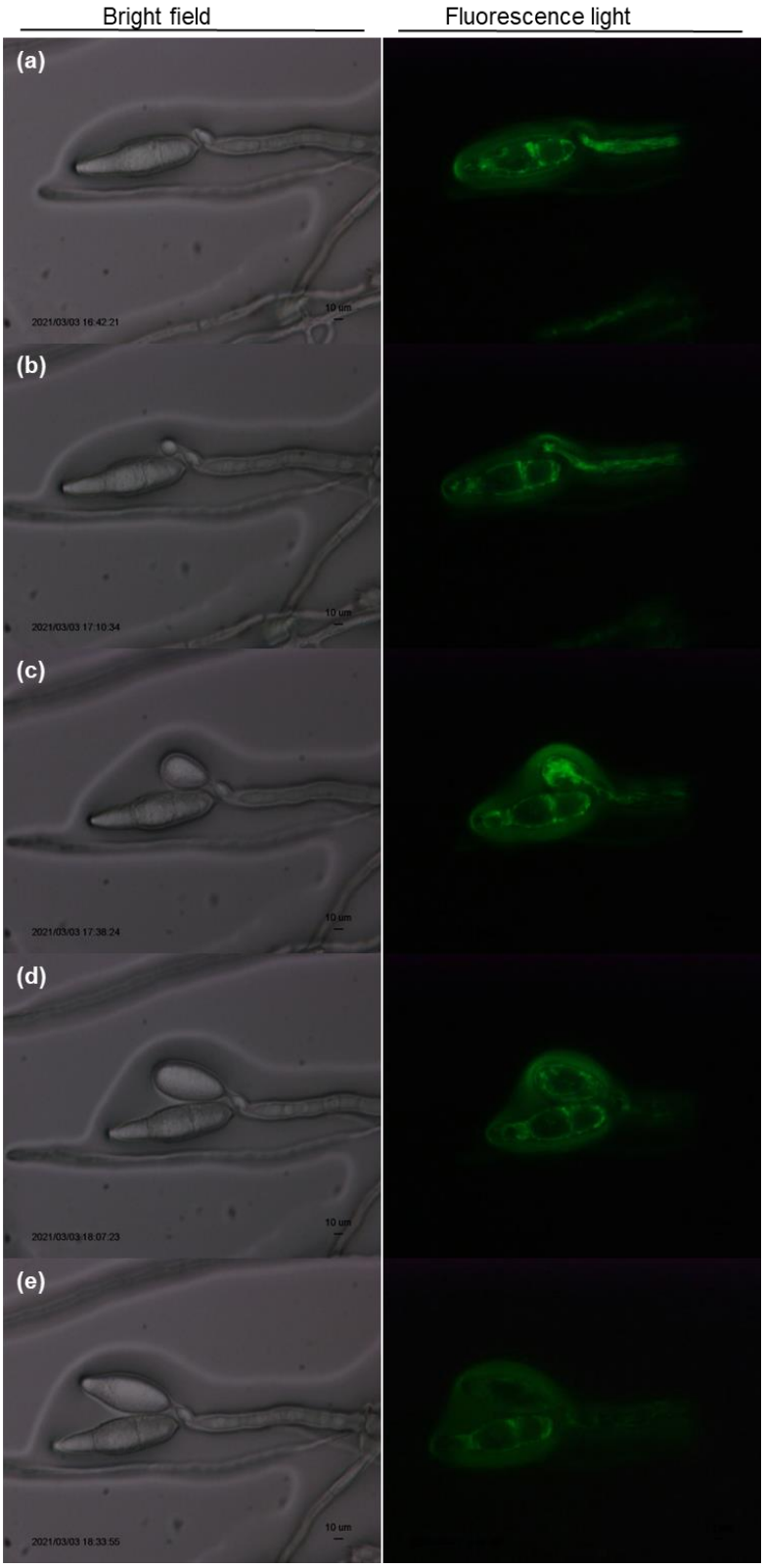

Figure 9 Mitochondrial movement and morphology during conidia development (a) at zero minute where the protuberance like structure appeared, mitochondria were tubular-

shaped and moving towards the edge of the protuberance (b) at 28 minutes, conidia became visible, tubular mitochondria were moving into the conidia (c) at 56 minutes, tubular mitochondria continued to move into conidia (d) at 86 minutes, tubular mitochondria have distributed throughout the conidium (e) at 112 minutes, movement of mitochondria has stopped and shape was changed into dot shape. Conidium was about to turned into two-celled conidium.

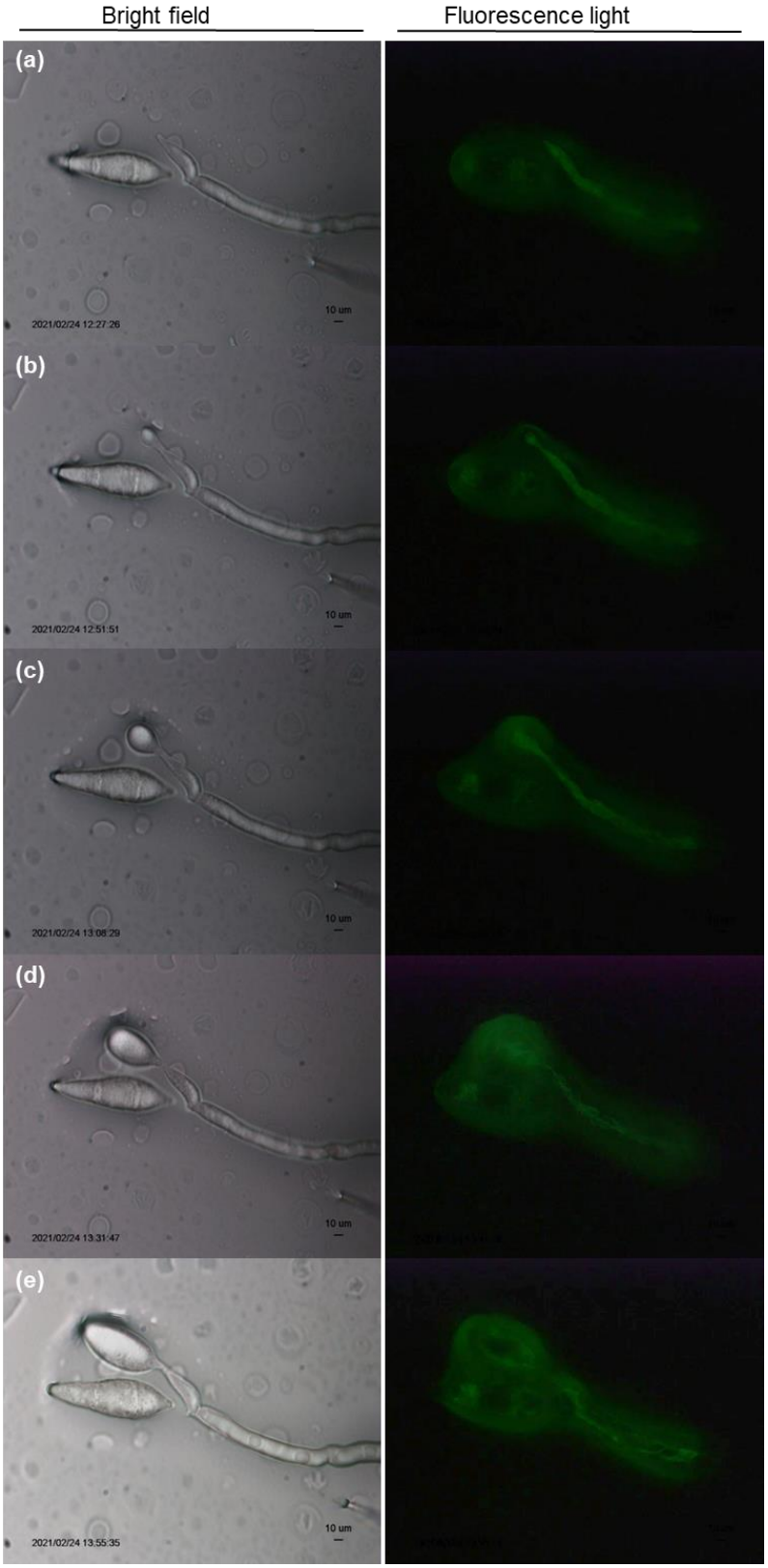
Bright field
Fluorescence light
(a)
2021/02/24 12:27:26
10 um
(b)
2021/02/24 12:51:51
10 um
(c)
2021/02/24 13:08:29
10 um
(d)
2021/02/24 13:31:47
10 um
(e)
2021/02/24 13:55:35
10 um

Figure 10 Mitochondrial movement and morphology during conidia development (a) at zero minute where the protuberance like structure appeared, mitochondria were tubular-shaped and moving towards the edge of the protuberance (b) at 24 minutes, conidia became visible, tubular mitochondria were moving into the conidia (c) at 41 minutes, tubular mitochondria continued to move into conidia (d) at 64 minutes, tubular mitochondria have distributed throughout the conidium (e) at 88 minutes, movement of mitochondria has stopped and shape was changed into dot shape. Conidium was about to turned into two-celled conidium.

2.4 Discussion

In this chapter, we discussed about the morphology of mitochondria in *P. oryzae* during the early conidiation using *CitA-GFP* system. Recently, Syib'li et al., (2020) visualized the morphology of the mitochondria in *P. oryzae* using laser-scanning confocal microscopy and found that the mitochondria of single celled baby-conidia are dot shaped and later develop into a network as conidia aged. In the present research, we found that, during the formation of protuberance like structure, the mitochondrial morphology is tubular-shaped and changed to dot-like shape simultaneously with septa formation, before the formation of two-celled conidia. Syib'li et al., (2020) reported that hyphal tips have dot mitochondria and older hyphae have tubular shaped, whereas in the present study we report mitochondria in conidiophore to be tubule. Tubular –shaped might be the specific morphology needed during the movement of the mitochondria. Osman et al., (2015) reported that in *Saccharomyces cerevisiae*, tubular mitochondria is distributed in the budding daughter cell and subsequently localize at the distal membrane. Therefore, we can state that both fungi might have similar conserved system for morphology and distribution of mitochondria. In *S cerevisiae,* the mitochondrial fission protein Fis1 has been found to be required for apoptosis and mitochondrial fragmentation (Madeo et al. 1999). The study on *MoFIS1, Fis1* ortholog of *P. oryzae,* has found that *MoFIS1* is important for growth, conidiation and virulence of *P. oryzae* (Khan et al. 2015; Zeng et al. 2014). *MoFIS1* in *P. oryzae* may be involved in morphology of mitochondria through regulating mitophagy (Zhong et al. 2016). This also highlights the linkage between mitochondrial fission and conidiation in *P. oryzae*. *MoFis1* may concern with the mitochondrial metamorphosis during the early conidiation that was identified in this report, but further analysis using *MoFis1* mutants with *CitA-GFP* system is required.

These findings will elucidate the mechanism of mitochondrial inheritance in *P. oryzae*, which is the key to solve the mechanism of QoI resistance distribution.

Chapter 3

ESTABLISHMENT OF REAL-TIME PCR PROTOCOL

3.1 Introduction

Quantitative polymerase chain reaction (q-PCR) or real-time PCR (RT-PCR) is a method by which the quantity of the PCR product is measured in real-time. This technique is very useful for investigating gene expression and quantification of alleles. In PCR, the amplified DNA product is known as amplicon. In conventional PCR the amplicon is detected after completion of all polymerase chain reaction cycles. On the contrary, RT-PCR, the amplicon accumulation is measured as the polymerase chain reaction progresses. Therefore, the term real time is used.

The amplicon quantification is done after each cycle by quantifying the fluorescent reporter molecule in each reaction well. The fluorescent yield increased with an increasing amount of amplicon. Popular fluorescent reporters used in RT-PCR are SYBR Green and TaqMan. SYBR Green can only bind to double-stranded DNA and when bound it emits around 1,000 times greater fluorescence than when it is free in solution. With an increasing number of amplicons, which is a dsDNA, the fluorescent signal from SYBR Green also increased (Tajadini et al., 2014). An alternative approach is use of TaqMan probes, which contain two fluorophores namely quencher and reporter. The quencher absorbs the signal from the reporter when both are at close proximity. Therefore, the quencher and reporter are placed in close proximity on the same short oligonucleotides in the PCR mix. During amplification, DNA polymerase activity separates the reporter

and quencher allowing them to set apart. This liberates the fluorescence. Using TaqMan probe is expensive yet sequence-specific amplification can be measured. In contrast, SYBR Green is a non-specific dsDNA-binding dye (Fraga et al., 2008).

RT-PCR allows determination of the initial number of copies of template DNA with high accuracy. It also can be used to make qualitative decisions such as the presence or absence of a sequence or to quantify copy number. In a typical amplification plot, the number of PCR cycles is shown on the x-axis, and the fluorescence is shown on the y-axis. There are two clear phases in the plot namely exponential phase and plateau. To reliably quantify a copy number a standard curve is used (Svec et al., 2015).

Using a standard curve allows us to estimate the DNA concentration of unknown samples. This is done by comparing the Ct value of the unknown sample to standards with known DNA concentrations. To prepare a standard curve a dilution series from a known concentration has to be made. The amount of fluorescent signal for each standard in the dilution series is measured and the Ct values are recorded. These Ct values are used to create the standard curve. Since Ct values are inversely proportional to the concentration of DNA, the higher concentration will give a lower Ct value. When the Ct values for each dilution are plotted on a graph, the standard curve can be generated using a simple regression line. Since the standards are 10-fold dilutions, the Ct from one standard to the next should be uniform. Standard curve is prepared using a log of the known standard concentrations in the X axis and Ct value of each standard in the Y axis. The slope of the plot measures the efficiency of the PCR reaction (Heid et al., 1996).

3.2 Methodology

3.2.1 Construction of qPCR standard plasmids for wild type and mutant alleles of *Cytb* to quantify *Cytb* allele

DNA extracted from plasmid with wild type sequence (3.224kbp) (pGem-T easy 3016bp+ insert 208bp) and Plasmid with mutant type sequence (3.189kbp) (pGem-T easy 3016bp+ insert 208bp) were used to prepare the standard curve. The dilution series (10^8,10^7,10^6,10^5,10^4,10^3,10^2 molecules/ µl) were prepared from both types of DNA.

3.2.2 Optimization of qPCR to quantify *cyt b* allele

Two different taq enzymes and PCR conditions were tested. Taq enzymes namely, SYBR Green ER qPCR SuperMix for ABIPRISM and Go Taq qPCR Master Mix were tested to optimize qPCR. Table 2 and 3 provides information on the pcr condition and the amount of the chemicals used with SYBR Green ER qPCR SuperMix for ABIPRISM.

Table 2. Composition of reaction mixture for q-RT-PCR (SYBR Green ER qPCR SuperMix for ABIPRISM)

Components	Amount (µl)
SYBR Green ER qPCR SuperMix	12.5
Primer F (10pmol/µl)	0.5
Primer R (10pmol/µl)	0.5
Template	1
SDW	10.5
Total	25

Table 3. Condition of reaction for qPCR (SYBR Green ER qPCR SuperMix for ABIPRISM)

Step	Temperature (°C)	Time (min)
Denaturation	50	2:00
Annealing	95	10:00
Extension	95	0:15 (40 cycles)
Final elongation	60	1:00

The conditions given below (Table 4 and 5) are used with Go Taq qPCR Master Mix. 40 PCR cycles were used in each condition and taq enzyme.

Table 4. Composition of reaction mixture for qPCR (Go Taq qPCR Master Mix)

Components	Amount (µl)
Go Taq qPCR Master Mix	12.5
Primer F (100pmol / µl)	0.5
Primer R (100pmol / µl)	0.5
Template	5
SDW	6.5
Total	25

Table 5. Condition of reaction for qPCR (Go Taq qPCR Master Mix)

Step	Temperature (℃)	Temperature (℃)	Time (min)
Denaturation	95	95	2:00
Annealing	95	95	0:15
Extension	60	60	1:00 (40 cycles)
Final elongation	60	60	1:00

3.2.3 Protoplast fusion to prepare the heteroplasmy fusant strain

To produce the heteroplasmy strain which contains the same amount of wild type (WT) and mutant type (MT) alleles, two strains 2013-131 (MT) and 2013-158 (WT) were fused using the protoplast-PEG method. protoplast isolation was done from mycelia which were initially started with a stock mycelium and incubated for around five days in 2YEG liquid medium (2 g/L yeast extract and 10 g/L glucose) at 27°C. The protoplast isolation was done by digesting the cell wall of the mycelia with the digestion enzyme mix (Yatalase 0.02g/ml and cellulose 0.005g/ml) followed by incubation at 37°C in a shaker for one hour. The mixture was then filtered through filter (Calbiochem), washed with isotonic buffer and centrifuged. The collected protoplast was resuspended in 300 µl of isotonic buffer. Mix the protoplast solution and add ice cool PEG solution. The mixture was kept on ice for 20minutes. After the PEG treatment, 30 ml of STC buffer was added and it was mixed gently. The mixture of protoplasts were centrifuged at 3500 rpm for 10minutes. 200 µl of STC buffer was added into the pellet. The protoplast solution was cultured in bottom agar (Yeast Nitrogen base w/o amino acid 6.7g/L, glucose 5g/L, sucrose 205g/L and agar 15g/L) for 24 hours. These colonies were again cultured on 24 well- micro plate of PA (Prune extract 4g, Lactose 5g, Yeast extract 1g,agar 17g) for 1 week.

Go Taq master mix (Promega) and was used for RT-PCR reaction. 96 well-plate was used for the reaction. The primer sequence is given Table 6.

Table 6: Primer list for amplification of wild type and QoI resistant type of cyt b allele

Name	Primer 5'- 3'
Wild F	ACATAGTAATACAGCTTCTGC
Wild R	AAGATTAGTAATAACTGTAGCA
Resistant F	GGACAGATGTCATTATGAGC
Resistant R	ACTAAAGCAGCTAATACAAAAG

3.2.4 Quantification of *Cytb* allele in heteroplasmy fusant and field isolates

Resistant and susceptible strains were collected from the fields in Akita and Hyogo prefectures. Two susceptible strains 2013-208 and 130s were collected from Hyogo prefecture and Akita prefecture respectively. Four resistant strains were also collected namely 2013- 156, 2013-131 (Hyogo prefecture), 128r, 132r (Akita prefecture).

These strains and two resultant strains from the fusent (strain 3 and 6) were used to quantify WT and MT variants of *Cytb* allele. The ratio of WT and MT alleles were calculated to detect the heterogeneity of the *Cytb* allele in WT and MT variants. Go Taq qPCR Master Mix (Promega) was used for the qPCR.

3.3 Results

3.3.1 Construction of qPCR standard plasmids for wild type and mutant alleles of *Cytb* to quantify *Cytb* allele

The concentration of wild type and mutant alleles are 1.25×10^{10} and 7.8×10^{9} respectively.

3.3.2 Optimization of qPCR method

SYBR Green ER qPCR SuperMix for ABIPRISM master mix showed slow rise in the amplification curve. Initially, it was tried with 10^{10}-10^{8} dilution series of wild type DNA and mutant type DNA. Dilution below 10^{4} and dilution above 10^{8} shows almost same Ct value and the standard curve was not generated accurately. 10^{8}-10^{4} could be used to generate standard curve but the amplification curve showed slow rise when this taq enzyme was used.

Go Taq qPCR Master Mix showed no difference in Ct value in between 10^{10}-10^{8} and 10^{4}-$10^{2.}$ Therefore, the dilutions between 10^{10}-10^{8} was used to generate the standard curve.

DNA extracted from wild type was used as the negative control for the Mutant type DNA and vice versa.

3.3.2 Quantification of *Cyt b* allele in heteroplasmy fusant

Table 7 Mean total copy number of WT and MT alleles per total DNA

Strain	Allele copy number / Total DNA 100 ng		
	WT	MT	WT : MT
3	$1.28x10^7$	$1.15x10^7$	1.11 : 1
6	$1.74x10^7$	$6.67x10^4$	2.61 : 1

Strain namely 3 and 6 has WT:MT ratio as 1.11: and 2.61:1 respectively (Table 7). Both of these strains showed heteroplasmy nature. These fusants were used as the control sample in next experiment to analyses the homoplasmy of mitochondria.

3.3.3 Quantification of C*yt b* allele in field isolates

Table 8 WT and MT allele copy number per total DNA and WT / MT ratio in sensitive and resistant strains

Strain	Phenotype	Allele copy number / Toatal DNA 100 ng		
		WT	MT	WT : MT
2013-156	Resistant	$5.79x10^{3}$	$7.87x10^{7}$	$1 : 1.36x10^{4}$
2013-208	Susceptible	$1.34x10^{5}$	$5.70x10^{1}$	$2.34x10^{3} : 1$
2013-131	Resistant	$2.87x10^{2}$	$5.23x10^{5}$	$1 : 1.82x10^{3}$
128r	Resistant	$1.86x10^{4}$	$1.73x10^{7}$	$1 : 9.27x10^{2}$
132r	Resistant	$7.80x10^{3}$	$4.67x10^{7}$	$1 : 5.98x10^{3}$
130s	Susceptible	$1.19x10^{10}$	$7.12x10^{3}$	$1.68x10^{6} : 1$

3.4 Discussion

A standard solution with a known number of copies with WT / MT allele was used to generate standard curve. Real-time could be used for the quantitative analysis of specific allele. The polymerase enzyme, effective quantification range, and most effective reaction conditions were finalized with this experiment. Dilution series of a known number of copies with WT / MT allele were used in optimization. Polymerase enzyme which is most appropriate for the present quantification system is Go Taq qPCR Master Mix, with an effective range of quantification 10^8-10^4. This system was used to quantify the WT / MT alleles of the strain in further experiments. We successfully created a heteroplasmy strain which has the same amount of both wild type and mutant type allele. This strain was used to understand the homoplasmy of *Pyricularia oryzae* in the next experiment.

Chapter 4

q-RT-PCR TO QUANTITY ISOLATES FOR THE HOMOPLASMY AND HETEROPLASMY CONDITION

3.1 Introduction

3.1.1 Mitochondrial inheritance and homoplasmy

Mitochondrial DNA (mtDNA) can easily undergo mutations than the nuclear DNA hence is it often mentioned that mtDNA can evolve quickly (Brown et al 1979). mtDNA is bi-parentally inherited but colonies prefer one type of mtDNA over other. *S. cerevisiae* is an excellent model organism to study about cellular and molecular pathways and has been used extensively to understand the molecular mechanisms of organelle inheritance. *S. cerevisiae* has most of the mitochondrial DNA as linear molecules of different length. The mitochondrial genome is packed into protein – DNA complexes known as nucleoids and *S. cerevisiae* has about 10-40 nucleoids per cell. The mitochondrial genome contains several of origins of replication but the role of mitochondrial RNA polymerase, Rp041 is still doubtful.

Segregation of cellular mechanism of mitochondrial DNA is largely unknown. In *S. cerevisiae,* it is hypothesized that retention of homoplasmy is influenced the fitness of the

allele to different environments and it also affects the nuclear sub nuclear genome in a cell (Hewitt et al 2020). During the sexual reproduction two haploid cells fuse to form a diploid cell. Zygote will have mixture of mitochondrial DNA if the parental cells have contributed different mitochondrial cells and this can also happen during the vegetative growth. This is termed as heteroplasmy. There are some evidences that says if mitochondrial DNA remain un-mix within few cell divisions, they become homoplasmic (Chen and Butow, 2005). Budding is known as multiplication of cells during asymmetric cell division. Mitochondrial DNA enters to the bud as soon as it emerges. Bud directed mitochondrial movement happens with the help of small fraction of mitochondrial DNA pool which is transferred from zygote to the bud and determines about the mitochondrial DNA type. Evidence suggests that bundle of actin cables along with myosin proteins are involved in the bud directed mitochondrial movement (Westermann 2014, Lazzarino et al 1994).

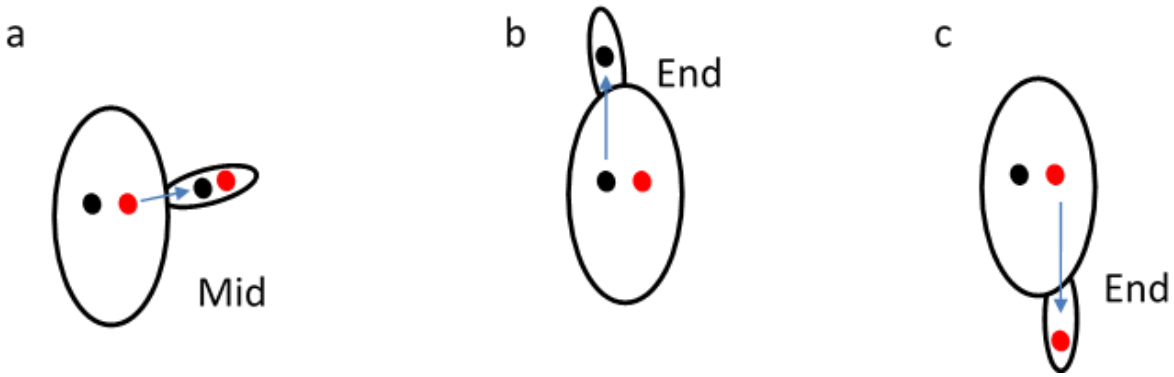

Figure 11 Mitochondrial distribution during budding in *S. cerevisiae.* **a.** Budding starting at the midpoint of the cell will have both the types of the parental mtDNA (Heteroplasmy). **b,c.** Budding starting at the either end of the cell will have one parental type mtDNA (Homoplasmy).

3.2 Methodology

The fused strain was first cultured in prune agar for 3days and then the small gel pieces were stored in 10% glycerol at -80^{0}C refrigerator for further use. The strain was taken out from 10% glycerol and cultured in 2YEG broth for around 5days at 25^{0}C.

3.2.1 Prepare samples without conidiation

One mycelium was taken out from the Liquid medium and then inoculated back into fresh 2YEG medium again. They were incubated for around 5days and those mycelia were used for protoplast isolation. The mycelia were filtered using mila cloth filter and the mycelia were transferred into pre-weighed falcon tube. The digestion enzyme mixture was pre-prepared and filtered using 0.4µm filter and injection tube. Digestion enzyme mixture was poured into mycelia and incubated at 37^{0}C at shaker for 2 hours. Then the mixture was filtered and washed with STC buffer. The supernatant was centrifuged at 3500g for 10minutes. After that, the pellet was collected and 500 µl of STC was added. Centrifugation step was repeated and the pellet was collected again. The protoplast was dissolved in 300µl of isotonic buffer. The number of cells was observed under hemocytometer for making the dilution series. The different dilution series were 10^1 ,10^2 ,10^3, 10^4 with isotonic buffer and 10^1 with SDW. The diluted protoplast was cultured on bottom broth agar at 25^{0}C for around 8 days to isolate single colonies. The single colonies were transferred into 2YEG broth and incubated at 25^{0}C for 5days. Later, the mycelia were filtered, freeze dried and processed with DNA extraction.

3.2.2 Prepare samples with conidiation

One mycelium was taken out from the Liquid medium and then inoculated into oatmeal agar medium. They were incubated for around 10-14 days and then scraped using scraper. The plates were incubated again for around 3 days and the condia were collected using 5ml of SDW. Conidia were diluted with SDW and the different dilution series of 10^1 ,10^2 ,10^3, 10^4 were prepared. Diluted conidia were cultured on water agar medium. After 4-5 days, single colonies were isolated and they were inoculated into 2YEG medium. Later, the mycelia were filtered, freeze dried and processed with DNA extraction.

3.2.3 Genomic DNA extraction

DNA was extracted by method explained by sone et al 1997. Briefly 0.05g of the sample was put into micro centrifuge tube with metal beads. Bead shocker was used at 2500rpm for 30sec and 500 µl of DNA extraction buffer was added. Phenol saturated with TE and 150µl Chloroform -isoamyl alcohol (24:1) was added. Then, it was centrifuged at 15,000rpm for 1hour. The upper layer was transferred into new micro centrifuge tube and 25µl of RNase A solution was added. The sample was incubated for 1 hour and later 500 µl of phenol was added. It was centrifuged for 5min at 15,000rpm. 250 µl of phenol and 250 µl of chloroform were added to the supernatant. Centrifugation was repeated. Then 500 µl of chloroform was added into the pellet before centrifugation. 500 µl of isopropanol was added and it was centrifuged at above mentioned condition. Later add 70% ethanol into the pellet and centrifuge for 5min at 15,000rpm. The supernatant was thrown and the pellet was dried in the dryer. Finally 50 µl of SDW was added to dissolve the pellet and OD value was checked before further using the DNA for q-RT- PCR.

3.2.4 q-RT- PCR

DNA extracted from plasmid with wild type sequence (3.224kbp) (pGem-T easy 3016bp+ insert 208bp) and Plasmid with mutant type sequence (3.189kbp) (pGem-T easy 3016bp+ insert 208bp) were used to prepare the standard curve. The dilution series (10^8,10^7,10^6,10^5,10^4 molecules/ µl) were prepared from both types of DNA. Three dilutions were prepared (10^1,10^2,10^3) from each unknown sample obtained from with conidiation and without conidiation process.

Go Taq master mix (Promega) was used for q-RT- PCR reaction. 96 well-plate was used for the reaction. Given below are the enzyme reaction mixture (Table 9) and q-RT- PCR condition (Table 10). The primer sequence is given Table 11.

Table 9: Enzyme reaction mixture

Compound	Amount
Master Mix	5 µl
Primer (each)	0.2 + 0.2 µl
CXR	0.1 µl
SDW	3.7 µl
DNA	1 µl
Total volume	10 µl

Table 10 q-RT-PCR conditions

Step	Temperature (℃)	Time (min)
Denaturation	95^0C	2 Minutes
Annealing	95^0C	0.15 Seconds
Extension	60^0C	1 Minutes
Final elongation	60^0C	1 Minutes

Table 11 Primer list for amplification of wild type and QoI resistant type allele

Name	Primer 5'- 3'
Wild F	ACATAGTAATACAGCTTCTGC
Wild R	AAGATTAGTAATAACTGTAGCA
Resistant F	GGACAGATGTCATTATGAGC
Resistant R	ACTAAAGCAGCTAATACAAAAG

3.3 Results

This experiment was conducted to reveal about homoplasmy condition *P oryzae.* The quantity of the allele *Cyt b* was measured using q-RT-PCR. The ratio of WT allele/MT allele was calculated and given in table 12. The isolates with conidiation showed homoplasmy with WT allele whereas samples with no conidiation showed heteroplasmy with both WT and MT allele.

Table 12 Ratio between wild type allele and resistant allele in colonies with *P. oryzae* with conidiation and with no-conidiation

Treatment	Sample Name	Mean quantity		WT:MT
		MT allele	WT allele	
Conidiation	c1.2	0.548	16473726	1: $3.32x10^{-8}$
	c2.1	160.546	54961719	1: $2.9x10^{-6}$
	c5.3	1.83	4920299.2	1: $3.71x10^{-7}$
	c6.2	405.326	9678236	1: $4.18x10^{-5}$
	c7.3	30.906	3583431.6	1: $8.62x10^{-6}$
	c8.2	165.015	23299954	1: $7.81x10^{-6}$
Non-conidiation	a.2	1872566	1661.04	$1:1.13x10^{3}$
	b.2	4014717	31048.364	$1:1.29x10^{2}$
	c.3	153160	575.494	$1:2.66x10^{2}$
	d.3	101443	465.922	$1:2.18x10^{2}$
	f.1	10.14	48415267	$1:2.09x10^{-7}$
	g.1	25.551	202843026	$1:1.26 x10^{-7}$
	1.3	424449	635.624	$1:6.68 x10^{2}$
Control	C	8647074	8484787.2	1:1.02

3.4 Discussion

Unlike nuclear genome, there are hundreds to thousand copies of mitochondrial DNA (mtDNA) in each cell. As a result of high frequency of mutagenesis, heteroplasmy is observed in a cell yet they quickly go back to homoplasmy after few sexual regeneration cycles or during vegetative cell growth (Ling et al 2011). In this chapter, we have shown our observations homoplasmy during asexual reproduction. We observed that the conidiation is the key to control homoplasmy during the asexual reproduction of *P. oryzae*. Previously it has been reported that a heteroplasmic *S. cerevisiae* strain obtained under laboratory conditions by mating Mat a and Mat α was segregate into homoplasmic progeny during zygote outgrowth. No selective pressure was used during the conidiation and yet after twenty generations all cells were homoplasmic (Dujon B 1981; Dujon B 2020). We also observed similar results that mitochondria will go back to homoplasmy after conidiation when there is no any stress (fungicide) is given. *Mhr1-1* a mitochondrial gene conversion gene deficient was isolated and characterized by Ling (1995) and later it was revealed that *Mhr 1* is essential for mtDNA partitioning into daughter cells (Ling 2002). It is also involved in the generation of homoplasmic progeny of heteroplasmic mtDNA (Ling 2004). *Mhr1-1* is a single amino acid replacement that might affect the homoplasmic progeny and it slower the generation of homoplasmic cells. Over expressed *Mhr1* enhanced the heteroplasmic cells (Ling 2004). In *P. oryzae* also, same gene might be involved in the maintenance of homoplasmicity.

Chapter 5

General Discussion

Pyricularia oryzae, is a filamentous ascomycete fungus which causes rice blast disease in rice. This pathogen has a host range of over 50 species including many economically important cereals and grasses (Schulze-Lefert and Panstruga, 2011). China, Korea, Japan, Vietnam and United States had to destroy 5.7million hectares of rice in 2001 to 2005 due to rice blast disease (Wilson and Talbot, 2009). *P. oryzae* can infect leaves, stems, nodes and panicles of rice which include all stages of development of the plant. QoI fungicide is widely used to control the disease and this created high resistance towards the fungicide. This fungicide affects complex III in TCA and single nucleotide mutation can help *P. oryzae* to develop resistance to the fungicide. Therefore it is important to understand about the mitochondrial morphology and mitochondrial inheritance during conidiation.

This study focused on mitochondria present in conidiaphore and their movement into conidia during condiation. We discussed about the morphology of mitochondria in *P. oryzae* during the early conidiation using *CitA-GFP* system. *P. oryzae* transformant with GFP-tagged Citrate synthase (*Cit A*) gene was used in this study. Strain Ina86-137 *CitA*-GFP was cultured on special slide for 30-33hours and observed under the microscope (Olympus BX 50). Initially, lower magnification was used to optimize the observation time and the observation point of the conidiophore. Later, higher magnification was used to observe the morphology and movement of mitochondria from protruberance to baby conidia. In the present research, we found that, during the formation of protuberance like

structure, the mitochondrial morphology is tubular-shaped and changed to dot-like shape simultaneously with septa formation, before the formation of two-celled conidia. Therefore we can state that tubular shape might be the specific morphology needed during the movement of the mitochondria from protuberance to conidia. Tubular mitochondria is distributed in the budding daughter cell and subsequently localized at the distal membrane in *Saccharomyces cerevisiae* (Osman et al 2015). Therefore, we can state that both fungi might have similar conserved system for morphology and distribution of mitochondria.

In next two experiments, quantitative real time polymerase chain reaction (q-RT-PCR) was used to quantify the *Cit b* allele. q-RT-PCR is a method by which the quantity of the PCR product is measured in real-time. This technique is very useful for investigating gene expression and quantification of alleles. Allele quantification system was first established with q-RT-PCR using wild type (WT) and Mutant type (MT) allele.

We observed that the conidiation is the key to control homoplasmy during the asexual reproduction of *P. oryzae*. There are multiple copies of mitochondrial DNA (mtDNA) in each cell and due to frequent mutagenesis, heteroplasmy is observed in cells with respect to mtDNA (Fritsch et al, 2014; Ling et al, 2011). In a fussed strain of *S. cerevisiae* obtained by mating Mat a and Mat α was also segregated into homoplasmic progeny. In our observations mtDNA was segregated into homoplasmy after conidiation in the absence of any stress such as fungicide. *Mhr1-1* a mitochondrial gene conversion gene deficient was isolated and characterized by Ling (1995). We believe that *Mhr1-1* might affect the homoplasmic progeny and it slower the generation of homoplasmic cells. Over

expressed *Mhr1* enhanced the heteroplasmic cells (Ling 2004). We concluded that in *P. oryzae* also, same gene might be involved in the maintenance of homoplasmicity.

REFERENCES

Asibi, A.E., Chai, Q. and Coulter, J.A., 2019. Rice blast: A disease with implications for global food security. *Agronomy*, *9*(8), pp.451.

Barker, R., Herdt, R.W. and Rose, B., 1985. The Rice Economy of Asia, Resources for the Future in Cooperation. *International Rice Research Institute, Washington, DC*. pp. 20-35.

Boddy, L. (2016). Pathogens of autotrophs. In S. C. Watkinson, N. Money, & L. Boddy (Eds.), *The Fungi* Academic Press. pp. 245–292

Brown, W.M., George, M. and Wilson, A.C., 1979. Rapid evolution of animal mitochondrial DNA. *Proceedings of the National Academy of Sciences*, *76*(4), pp.1967-1971.

Castroagudín, V.L., Ceresini, P.C., de Oliveira, S.C., Reges, J.T., Maciel, J.L., Bonato, A.L., Dorigan, A.F. and McDonald, B.A., 2015. Resistance to QoI fungicides is widespread in Brazilian populations of the wheat blast pathogen *Magnaporthe oryzae*. *Phytopathology*, *105*(3), pp.284-294.

Chen, M., Wang, B., Lu, G., Zhong, Z. and Wang, Z., 2020. Genome Sequence Resource of *Magnaporthe oryzae* Laboratory Strain 2539. *Molecular Plant-Microbe Interactions*, *33*(8), pp.1029-1031.

Chen, X.J. and Butow, R.A., 2005. The organization and inheritance of the mitochondrial genome. *Nature Reviews Genetics*, *6*(11), pp.815-825.

Couch, B.C. and Kohn, L.M., 2002. A multilocus gene genealogy concordant with host preference indicates segregation of a new species, *Magnaporthe oryzae*, from *M. grisea*. *Mycologia*, *94*(4), pp.683-693.

Dean, R.A., Talbot, N.J., Ebbole, D.J., Farman, M.L., Mitchell, T.K., Orbach, M.J., Thon, M., Kulkarni, R., Xu, J.R., Pan, H. and Read, N.D., 2005. The genome sequence of the rice blast fungus *Magnaporthe grisea*. *Nature*, *434*(7036), pp.980-986.

Dujon, B., 2020. Mitochondrial genetics revisited. *Yeast*, *37*(2), pp.191-205.

Fernandez, J. and Orth, K., 2018. Rise of a cereal killer: the biology of *Magnaporthe oryzae* biotrophic growth. *Trends in microbiology*, *26*(7), pp.582-597.

Fraga, D., Meulia, T. and Fenster, S., 2008. Real-time PCR. *Current protocols essential laboratory techniques*, (1), pp.10-3.

Glancy, B., 2020. Visualizing mitochondrial form and function within the cell. *Trends in molecular medicine*, *26*(1), pp.58-70.

Goh J, Jeon J, Lee Y.H., 2017 ER retention receptor, *MoERR1* is required for fungal development and pathogenicity in the rice blast fungus *Magnaporthe oryzae*. Sci Rep 7:1259.

Han JH, Shin JH, Lee YH, Kim KS (2018) Distinct roles of the *YPEL* gene family in development and pathogenicity in the ascomycete fungus *Magnaporthe oryzae*. Sci Rep 8:14461.

Hayashi, K., Suzuki, F. and Hayano-Saito, Y., 2017. Multiplex PCR assay for simultaneous detection of MBI-D and Q o I resistance in rice blast fungus. *Journal of General Plant Pathology*, *83*(5), pp.304-309.

Heid, C.A., Stevens, J., Livak, K.J. and Williams, P.M., 1996. Real time quantitative PCR. Genome research, 6(10), pp.986-994.

Hewitt, S.K., Duangrattanalert, K., Burgis, T., Zeef, L.A., Naseeb, S. and Delneri, D., 2020. Plasticity of mitochondrial DNA inheritance and its impact on nuclear gene transcription in yeast hybrids. *Microorganisms*, *8*(4), p.494.

Ishi, K., Maruyama, J.I., Juvvadi, P.R., Nakajima, H. and Kitamoto, K., 2005. Visualizing nuclear migration during conidiophore development in *Aspergillus nidulans* and *Aspergillus oryzae*: multinucleation of conidia occurs through direct migration of plural nuclei from phialides and confers greater viability and early germination in *Aspergillus oryzae*. *Bioscience, biotechnology, and biochemistry*, *69*(4), pp.747-754.

Ishii, H., 2006. Impact of fungicide resistance in plant pathogens on crop disease control and agricultural environment. *Japan Agricultural Research Quarterly: JARQ*, *40*(3), pp.205-211.

Ishii, H., 2015. Rice pathogens in Japan. In *Fungicide Resistance in Plant Pathogens*. Springer, Tokyo. pp. 341-354

Jensen, R.E., Aiken Hobbs, A.E., Cerveny, K.L. and Sesaki, H., 2000. Yeast mitochondrial dynamics: fusion, division, segregation, and shape. *Microscopy research and technique*, *51*(6), pp.573-583.

Kain, S.R., Adams, M., Kondepudi, A., Yang, T.T., Ward, W.W. and Kitts, P., 1995. Green fluorescent protein as a reporter of gene expression and protein localization. *Biotechniques*, *19*(4), pp.650-655.

Kou, Y., He, Y., Qiu, J., Shu, Y., Yang, F., Deng, Y. and Naqvi, N.I., 2019. Mitochondrial dynamics and mitophagy are necessary for proper invasive growth in rice blast. *Molecular plant pathology*, *20*(8), pp.1147-1162.

Lackner, L.L., 2014. Shaping the dynamic mitochondrial network. *BMC biology*, *12*(1), p.35.

Lazzarino, D.A., Boldogh, I., Smith, M.G., Rosand, J. and Pon, L.A., 1994. Yeast mitochondria contain ATP-sensitive, reversible actin-binding activity. *Molecular biology of the cell*, *5*(7), pp.807-818.

Li D, Calderone R (2017) Exploiting mitochondria as targets for the development of new antifungals. Virulence 8(2):159–168.

Ling, F., Makishima, F., Morishima, N., Shibata, T., 1995 A nuclear mutation defective in mitochondrial recombination in yeast. *EMBO J.* , *14*, pp.4090–4101.

Ling, F., Mikawa, T. and Shibata, T., 2011. Enlightenment of yeast mitochondrial homoplasmy: diversified roles of gene conversion. *Genes*, *2*(1), pp.169-190.

Ling, F., Shibata, T., 2002 Recombination-dependent mtDNA partitioning. In vivo role of Mhr1p to promote pairing of homologous DNA. *EMBO J.* , *21*, pp.4730–4740.

Ling, F., Shibata, T., 2004 Mhr1p-dependent concatemeric mitochondrial DNA formation for generating yeast mitochondrial homoplasmic cells. *Mol. Biol. Cell* , *15*, pp.310–322.

Lorang, J.M., Tuori, R.P., Martinez, J.P., Sawyer, T.L., Redman, R.S., Rollins, J.A., Wolpert, T.J., Johnson, K.B., Rodriguez, R.J., Dickman, M.B. and Ciuffetti, L.M., 2001. Green fluorescent protein is lighting up fungal biology. *Applied and Environmental Microbiology*, *67*(5), pp.1987-1994.

Martínez-Reyes, I. and Chandel, N.S., 2020. Mitochondrial TCA cycle metabolites control physiology and disease. *Nature communications*, *11*(1), pp.1-11.

Mendoza, H., Perlin, M.H. and Schirawski, J., 2020. Mitochondrial Inheritance in Phytopathogenic Fungi—Everything Is Known, or Is It?. *International Journal of Molecular Sciences*, *21*(11), p.3883.

Miyagawa, N., Fuji, M. and Kawabata, Y., 2013. Occurrence of orysastrobin-resistant isolates of rice blast fungus. *Jpn J Phytopathol*, *79*, pp.197.

Nalley, L., Tsiboe, F., Durand-Morat, A., Shew, A. and Thoma, G., 2016. Economic and environmental impact of rice blast pathogen (*Magnaporthe oryzae*) alleviation in the United States. *PloS one*, *11*(12), p.e0167295.

Perez-Nadales, E., Nogueira, M.F.A., Baldin, C., Castanheira, S., El Ghalid, M., Grund, E., Lengeler, K., Marchegiani, E., Mehrotra, P.V., Moretti, M. and Naik, V., 2014. Fungal model systems and the elucidation of pathogenicity determinants. *Fungal genetics and biology*, *70*, pp.42-67.

Rahnama, M., Phillips, T.D. and Farman, M.L., 2020. First report of the blast pathogen, *Pyricularia oryzae*, on *Eragrostis tef* in the United States. *Plant Disease*, *104*(12), p.3266.

Rizzuto, R., Brini, M., Pizzo, P., Murgia, M. and Pozzan, T., 1995. Chimeric green fluorescent protein as a tool for visualizing subcellular organelles in living cells. *Current biology*, *5*(6), pp.635-642.

Schulze-Lefert, P. and Panstruga, R., 2011. A molecular evolutionary concept connecting nonhost resistance, pathogen host range, and pathogen speciation. *Trends in plant science*, *16*(3), pp.117-125.

Sesma, A. and Osbourn, A.E., 2004. The rice leaf blast pathogen undergoes developmental processes typical of root-infecting fungi. *Nature*, *431*(7008), pp.582-586.

Suelmann, R. and Fischer, R., 2000. Mitochondrial movement and morphology depend on an intact actin cytoskeleton in *Aspergillus nidulans*. *Cell motility and the cytoskeleton*, *45*(1), pp.42-50.

Svec, D., Tichopad, A., Novosadova, V., Pfaffl, M.W. and Kubista, M., 2015. How good is a PCR efficiency estimate: Recommendations for precise and robust qPCR efficiency assessments. *Biomolecular detection and quantification*, *3*, pp.9-16.

Syib'li, M.A., Kodama, A., Abe, A. and Sone, T., 2020. Three-dimensional visualization of mitochondria in conidia of *Pyricularia oryzae* using green fluorescent protein (GFP) fused with citrate synthase (CitA). *Journal of General Plant Pathology*, *86*, pp.250-256.

Tajadini, M., Panjehpour, M. and Javanmard, S.H., 2014. Comparison of SYBR Green and TaqMan methods in quantitative real-time polymerase chain reaction analysis of four adenosine receptor subtypes. *Advanced biomedical research*, *3*.

Viana, M.P., Lim, S. and Rafelski, S.M., 2015. Quantifying mitochondrial content in living cells. *Methods in cell biology*, *125*, pp.77-93.

Westermann, B., 2014. Mitochondrial inheritance in yeast. *Biochimica et Biophysica Acta (BBA)-Bioenergetics*, *1837*(7), pp.1039-1046.

Wilson, R.A. and Talbot, N.J., 2009. Under pressure: investigating the biology of plant infection by *Magnaporthe oryzae*. *Nature Reviews Microbiology*, *7*(3), pp.185-195.

Zhu, D., Kang, H., Li, Z., Liu, M., Zhu, X., Wang, Y., Wang, D., Wang, Z., Liu, W. and Wang, G.L., 2016. A genome-wide association study of field resistance to *Magnaporthe oryzae* in rice. *Rice*, *9*(1), pp.1-9.

ACKNOWLEDGEMENT

I sincerely express my gratitude to my supervisor, Professor Teruo Sone, Research Faculty of Agriculture, Hokkaido University for his unstinted support. His infinite passion on research, style of student supervision and kind words, always motivated me to become a scientist like him.

I also truly grateful to Dr Ayumi Abe, Applied Molecular Microbiology Laboratory, Graduate School of Agriculture, Hokkaido University for his kind advice and assistance rendered me during this period.

I would like to extend my sincere thanks to all my labmates at Applied Molecular Microbiology Laboratory, who extended their support whenever I needed.

I owe a deep sense of gratitude to my husband, Wikum Harshana Jayasinghe and my daughter, Nathsuki Shehansa Jayasighe for supporting me to achieve my goals.